Increasing the efficiency Proton exchange membrane (PEMFC) & other fuel cells through multi graphene layers including polymer membrane electrolyte

Azin Chitsazan[a], Majid Monajjemi[b*]

[a]*Department of Chemistry, Science and research Branch, Islamic Azad University, Tehran, Iran.*

[b]*Department of Chemical engineering, Central Tehran Branch, Islamic Azad University, Tehran, Iran*

maj.monajjemi@iauctb.ac.ir

Keywords: *PEM fuel cells, parameter modelling and simulation, graphene, Langmuir adsorption.*

Multi layers Graphene has been simulated theoretically for hydrogen storage and oxygen diffusion at a single unit of fuel cell. Ion transport rate of DFAFC, PAFC, AFC, PEMFC, DMFC and SOFC fuel cells have been studied. AFC which uses an aqueous alkaline electrolyte is suitable for temperature below 90 degree and is appropriate for higher current applications, while PEMFC is suitable for lower temperature compared to others. Thermodynamic equations have been investigated for those fuel cells in viewpoint of voltage output data. Effects of operating data including temperature (T), pressure (P), proton exchange membrane water content (λ) , and proton exchange membrane thickness on the optimal performance of the irreversible fuel cells have been studied.Obviously, the efficiency of PEMFC extremely related to amount of the H_2 concentration, water activities in catalyst substrates and polymer of electrolyte membranes, temperature, and such variables dependence in the direction of the fuel and air streams.

Introduction

Generally, the fuel cells convert the chemical energies of a fuel (mostly H_2) and an oxidizing agent (usually oxygen in the air) into electricity through a pair of redox reactions. Although there are several kinds of fuel cells, customarily they all consist of, a cathode, an anode, and an electrolyte which allows ions, frequently positively protons (H^+) to move between two sides of the fuel cells .Brief ly, at the anode via a catalyst material and oxidation reaction, ions are generated through electrolytes which move toward the cathode. Simultaneously, in a reverse direction, electrons flow towards the cathode via an external circuit. At the cathodes, various catalysts can be applied to produce ions, electrons, and oxygen for reacting and forming water or some other products. Fuel cells are categorized based on species of their electrolytes and also by the difference in startup time ranging between around one second for PEMFC to ten minutes for solid oxide fuel cells (SOFC) with

maximum efficiency among 45% to 60%. In the fuel cell of a solid acid electrolyte, H^+ conducting oxyanion salt (solid acid) consists of a solid supported within the membrane which is saturated with H_2O for any further ions transporting. Anode reaction is: $H_2 \rightarrow 2H^+ + 2e^-$ and Cathode reaction is: $1/2\ O_2 + 2e^- + 2H^+ \rightarrow H_2O$ and the overall reaction is: $H_2 + 1/2\ O_2 \rightarrow H_2O$. In viewpoint of mechanism, at the anode, H_2 first come into contact with a nickel catalyst and break apart, bonding to the nickel surface forming weak H-Ni bonds consequently the oxidation reaction can be proceed. Each H_2 releases its electron, which moves around the external circuit to the cathode which is electrical current. Then the H^+ bonds with H_2O on the membrane surface for forming H_3O^+ that moves through the membrane to the cathode electrode, leaving the nickel catalyst for the next H_2. In H_2/O_2 fuel cells, two half- cell reactions accomplish simultaneously including, loss of electrons (an oxidation reaction) and gain of electrons (a reduction reaction) in anode and anode electrodes respectively. These processes make up the formation of water from hydrogen and oxygen gases through the total redox reaction of this fuel cell [1-3]. The electrolyte in the fuel cell consists of a solid acid supported within the membrane which is saturated with H_2O for any further ions transporting[1-5]. Anode reaction: $H_2 \rightarrow 2H^+ + 2e^-$ and Cathode reaction: $1/2\ O_2 + 2e^- + 2H^+ \rightarrow H_2O$ with an overall reaction: $H_2 + 1/2\ O_2 \rightarrow H_2O$ **.** In viewpoint of mechanism, at the anode, H_2 first come into contact with a nickel catalyst and break apart, bonding to the nickel surface forming weak H-Ni bonds consequently the oxidation reaction can be proceed. Each H_2 releases its electron, which moves around the external circuit to the cathode which is electrical current. Then the H^+ bonds with H_2O on the membrane surface for forming H_3O^+ that moves through the membrane to the cathode electrode, leaving the nickel catalyst for the next H_2. At the cathode, O_2 come into contact with nickel catalyst on the electrode surface and break apart bonding to the nickel sheet forming weak O-Ni bonds, enabling the reduction reaction to proceed. O_2 then leaves the nickel catalyst site, combining with two electrons that move in external circuit and two protons which have moved through the membrane for forming H_2O. Increasing the H_2 storage is a major section for the transition more and more hydrogen molecules in a fuel cell [2, 3].

PEMFC & other fuel cells

For both Phosphoric acid fuel cells (PAFC) and polymer electrolyte membrane fuel cells (PEMFC) (Table 1) , the H_2 molecules splitting at the anode into H^+ and transport across the electrolyte to the cathode.

Table 1. Fuel Cell Types.

Fuel cell	Electrolyte Use	Operating temperature	Efficiency Cell	Statues
DFAFC	Polymer membrane	$<40^0$	<40%	Commercial Research
AFC	Aqueous alkaline	$<90^0$	60%-70%	Commercial Research
DMFC	Polymer membrane	90-120	20-30%	Commercial Research
PEMFC	Polymer membrane	50-100 (Nafion) 120-200 (PBI)	25-40%	Commercial Research
Direct carbon fuel cell	Several different	700-900	70%	Commercial Research
Magnesium air fuel cell	Salt water	-25-50	90%	Commercial Research
Protonic ceramic fuel cell	H^+ conducting ceramic	700		Research
Enzymatic Biofuel Cells	not denature the enzyme	<40		Research
Phosphoric acid fuel cell	Molten (H_3PO_4)	150-200	45%	Commercial Research

For a PEMFC of static electrolyte with 25cm^2 active area, 50µm thickness and $9{\cdot}10^{-7}$cm$^2{\cdot}$s^{-1} diffusion coefficient of H+ ions [4-6], current density obtained for applied potential difference between 0.5-1.0V at 75°C exhibited in Fig.1 . Although PEMFC has a lower current than PAFC, due to its lower operating temperature allowing fast startup and can be applied in automotive power applications.

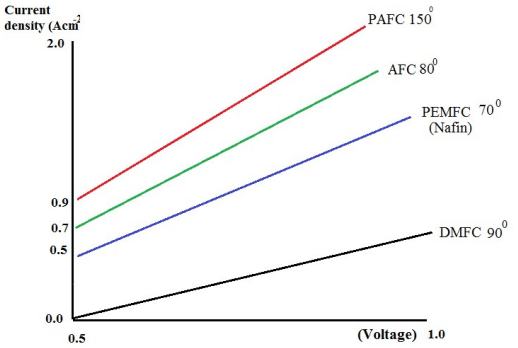

Figure 1. Current densities versus potential.

Another advantage of PEMFC is that its electrolyte is a solid material and is less expensive to manufacture than the liquid electrolyte $\eta(T,P) = \left(\frac{\Delta H - T\Delta S}{nF}\right) + RTLn\left(\frac{P_{H_2}P_{O_2}^{0.5}}{P_{H_2O}}\right)$ [25,26]. It is notable that, the maximum electrical energies and the potential differences are achieved when the fuel cells are operating under the thermodynamically reversible condition. Practically, an open circuit potential is considerably lower than the theory due to three main losses which are, first concentration polarizationV_{concen} second activation polarizationV_{act}, and third ohmic polarizationV_{ohmic}. The irreversible voltage loss V_{irrev} is a summation of these three parameters,$V_{irrev} = V_{act} + V_{ohmic} + V_{concen}$. Based on Butler-Volmer equation, a specific potential is needed for overcoming to the energies barriers which called activation polarization $i = I_c + I_A = i_0\left[-\exp(-\frac{\alpha_C nF\eta}{RT}\right) + \exp(\frac{\alpha_A nF\eta}{RT})]$ where $I_A\ and\ I_c$ are anode and cathode current densities, respectively and $i_0$is the reaction exchange currents densities. Meanwhile α_A and α_C are the charge transfer coefficients at the anode and cathode and n is the number of exchange protons per mole of reactant. Here η is the activation over potential term or $\Delta V_{act} = \eta = -\frac{RT}{n\alpha_C F} ln\frac{i}{i_0}$. For a fuel cell operating with a transfer coefficient of 0.45 activation losses versus current density are shown in Fig. 2.

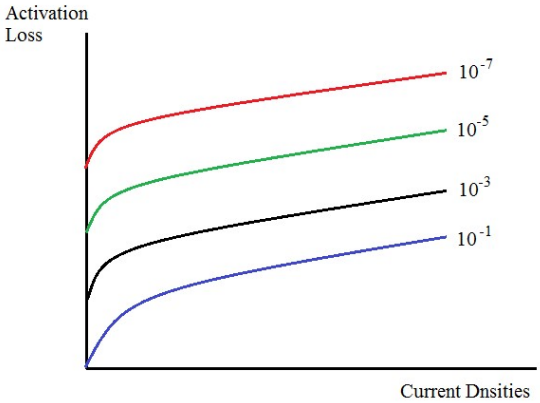

Figure 2. Activation loss as a function of current densities.

In addition two electrons from above equations (1&2) reach to the cathode electrode over the bipolar plates and over an external circuit. It is

notable that this mechanism is known as electro-osmotic drag. On the cathode electrode, oxygen gases diffuse to the catalyst layer and chemically combined with protons and electrons to form water (ORR). Obviously, the electrodes must be selected of porous materials that facilitate water moving to outside and the excess oxygen gases might be help for pushing water out of the cell (scheme 1& 2)[5-7]. Efficiency, permanence and cost reduction effort are the most important items for PEM fuel cells that cover construction and assembly methods [8]. There are several major items for increasing the life cycle and PEM fuel cells efficiency which are thermal management, water management, new catalysts, and novel material of membranes and also quality of electrodes. Operating conditions and operating strategies play an important role in a fuel cell lifecycle. Bad distribution of fuel cell reactants can appear in the presence of high cell currents, liquid water, fuel impurities, and different flows of fuel due to the sudden changes in the power demand and conditions between cell inlet and outlet.

In other hand, fuel starvation can cause severe degradation during of gross fuel starvation that cell voltages can become negative (as the anode) and the carbon is consumed given the lack of fuel, consequently anodic current will be provided by carbon corrosion to form carbon dioxide [9] . In addition, oxygen starvation can result in generation of hydrogen in the cathode or oxygen in the anode similarly during oxygen starvation the reaction at the cathode will produce hydrogen. For avoiding these problems the suitable monitoring controlling sensors and indicators are needed [10]. Several studies have shown that thermal management is important, higher temperature might be producing the radicals consequently the electrochemical surface area (ECSA) decrease the life time.

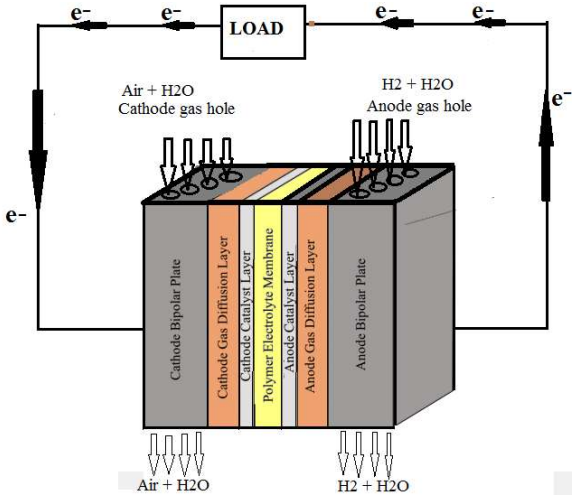

Scheme 1. One unit of PEM fuel cell structure

There are various cooling methods for PEM fuel cells which one important has been investigated by Fly [11] among Liquid- cooled air-cooled and evaporative-cooled fuel cells. Water management is essential and most important issues in PEM fuel cell technologies which dependent to adequate membrane hydration and avoidance of water flooding in the catalyst layers. It is important to keep the membrane and the catalyst layer humidified for high proton conductivity. In the presence of H_2O, the protons produce H_3O+ on the boundaries of the catalyst layer and the membrane which prevent of the proper activity of the protons from the anode catalyst layer to the cathode catalyst layer in

aqueous phase [4]. Therefore, tuning humidification of the membranes is also a basic way of cell performance while accumulation of too much water also impacts performance and lifetime [12].

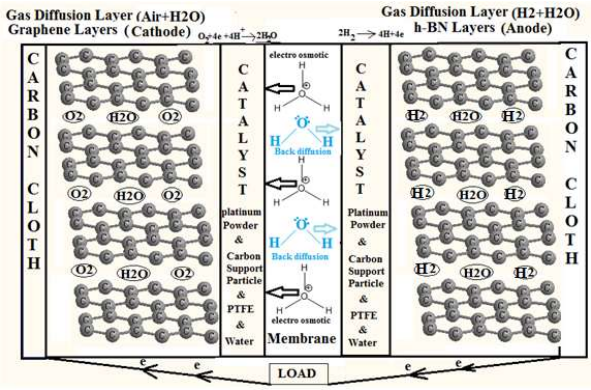

Scheme 2. Schematic model of all layers including two graphene layers and their activities in a whole unit of the fuel cell

Excess water blockages can instantly lead to reactant starvation and water flooding is an important limiting factor of PEM fuel cell efficiency and life time. Flooding appears in both cathode and anode electrodes [13] with three mechanisms as; (a) Water generated in the cathode side of the membrane by the electrochemical reaction (ORR), (b) electro-osmotic drag and (c) over-humidified reactant gases. Anode flooding is much longer than the cathode flooding. Although flooding in the cathode is much common compared to anode, flooding on the anode side of the membrane can also have serious consequences on the operation, performance and degradation and due to low fuel flow rates, removing H_2O from anode is much more difficult compared to cathode. Pasaogullari has reported, anode flooding is most probable for happening at low current, low reactant flow rates and low temperatures due to the lower electro-osmotic forces [14]. In other words proton flux is large in the anode electrode; therefore a strong electro-osmotic force pulls the H_2O from anode to cathode (due to the low water content). In contrast to the inlet of the anode side, at the exit current density is lower and H_2 concentration has decreased, so, the partial pressure of water is high and closer to total anode pressure [15-17]. Several researchers have assessment various tactics and technics for water managing. He et al. [18] associated partial pressure straightly to the flooding level and considered it to be a suitable indicator for efficiency. They planned a tool for monitoring the flooding measure in PEM fuel cell with inters digitized flow field. Diperno and coworkers [19] record a USA patent for a simple way which monitors the pressure drop across the flow field to detect flooding in PEM fuel cells. Problem of membrane dehydration is related to drying out in anode which causes a protonic resistance and consequently collapse in cell voltage. Therefore in dried situation radicals will produce and increased, to enhanced membrane degradation [20]. Anode dehydration is might be serious both at the inlet of the cell and at the outlet trajectory. In addition due to dehydrating conditions, the membrane leads to lower diffusion. One of the main reasons for dehydration is the strong electro-osmotic forces in the condition of high current densities where water replenishment by reactant humidification

or back-diffusion is not quick enough to cope with the lack of water [21].

Theoretical Background

The enthalpy of hydrogen combustion reaction or hydrogen heating amount for one mole of hydrogen can be calculated via $\Delta H = \Delta H_f^0(H2O) - \Delta H_f^0(H2) - \frac{1}{2}\Delta H_f^0\ (O2) = -286.31\ Kj/mol$. Hydrogen heating amounts are used as a measure of energies input for the fuel cells and this is the maximum value of thermal energy which can be extracted from hydrogen. In addition Gibbs free energy is given by the following equation: ΔG = ΔH - TΔS. which the difference between entropies of products and reactants can be calculated as $\Delta S = \Delta S_f^0(H2O) - \Delta S_f^0(H2) - \frac{1}{2}\Delta S_f^0(O2)$. The maximum electrical work is:$W_{max} = -n(emf)F$ = -ΔG where F is Faraday's constant and "emf" is the ideal electro motor force or potential of the cell. Therefore the theoretical hydrogen/oxygen fuel cell potential or maximum voltage of fuel cells is: $emf = E = \frac{-\Delta G}{nF} = \frac{237.342\ J\ mol^{-1}}{2*98486.5\ Coulmb} = 1.231\ Volt$ [22] .The thermal efficiency is defined based on amount of useful energy released when a fuel is reacted with an oxidant (ΔG), relative to the change in stored chemical energy (ΔH) therefore The maximum theoretical yields in a fuel cell is $\eta = \frac{\Delta G}{\Delta H} = \frac{237.342}{-28\ .31} = \%82.9$ [5]. Based on Nernst equation a function of temperature and pressure can be applied for any fuel cells as; $emf = E_{(T,P)} = -\left(\frac{\Delta H}{nF} - \frac{T\Delta s}{nF}\right) + \frac{RT}{nF} Ln\left[\frac{P_{H_2} P_{O_2}^{0.5}}{P_{H2O}}\right]$, **(1)** based on this equation, in an open circuit with reactant gases the actual cell potential is decreased (usually less than 1V) and it is called open circuit voltage (OCV) . This decreasing of actual cell potential is due to irreversible losses and hydrogen crossover losses which often called polarization, over potential, or over voltage including activation polarization, ohmic polarization and concentration polarization [23]. Activation polarization is associated with sluggish electrode kinetics which happens at both anode and cathode which can be expressed with Tafel equation: $\Delta V_{act} = \frac{RT}{\alpha F} ln \frac{i}{i_0}$ **(2)** where α is the electron transfer coefficient of the reaction at the electrodes and i0 is the exchange current density. The ohmic polarization appears due to resistance against the flow of protons in the electrolyte and also resistance to the flow of electrons through the electrode materials as the equation $\Delta V_{ohm} = i\Omega$ where i is the current flowing through the cell and Ω is the total cell resistances consist of electronic, ionic and contact resistance [9]. Concentration polarization is due to loss of potential because of inability of the surrounding material for maintaining the initial concentration of the bulk fluid, thus, a concentration gradient is formed. $\Delta V_{conc} = \frac{RT}{nF} \ln\left[\frac{i_L}{i_L - i}\right]$, That i_L is the limiting current. The actual cell voltage can be written as: V_{cell}=$E(T,P) - (\Delta V_{act} + \Delta V_{conc})_a - (\Delta V_{act} +$

$\Delta V_{conc})_c - \Delta V_{ohm}$ **(3)** by replacing the above equations in this equation the fuel cell polarization curve is: $V_{cell}=E(T,P) - \frac{RT}{\alpha_c F} ln \frac{i}{i_{0,c}} - \frac{RT}{\alpha_a F} ln \frac{i}{i_{0,a}} - \frac{RT}{nF} \ln \left[\frac{i_{L,a}}{i_{L,a}-i}\right] - \frac{RT}{nF} \ln \left[\frac{i_{L,C}}{i_{L,C}-i}\right] - i\Omega$. **(4)** Due to the activation energy barriers the polarization terms voltage collapse very fast and in the ohmic term polarization voltage falls slower due to the membrane and electrode ohmic resistance.

Modelling and simulation

The details mechanism of the PEMFC are very complex due to the different and tightly phenomenon which occur within a cell-fluid-dynamic, migration, electro chemical reaction, diffusions, water transports inside polymer membrane involving both electro-osmotic drag and back diffusion, proton transports via proton-conductivities of the polymer membranes, electron conduction via electrically conductivities of the cell components, heat transfer involving both conduction via solids components of the cells and convection of reactant gases and cooling medium, water transports both evaporation and liquids via porous catalyst layer, gas diffusion layer , and phase changes (scheme 3). including graphene and cell Modelling is needed for describing the basically phenomenon to evaluate the cells steady-state and dynamic behavior. However, the complex mechanism inside the fuel cell causes challenging in some models involving reactants, cooling, and humidification and conditioning systems.

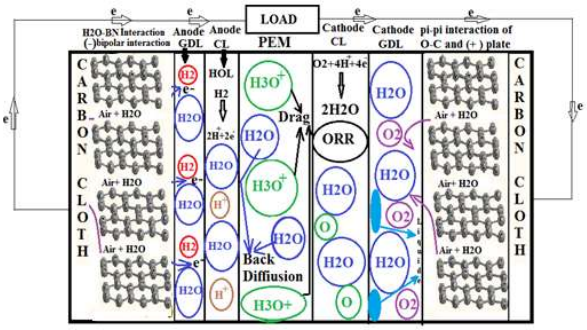

Scheme3. Processing and operating of a PEM fuel cell

Models are able to predict fuel cell efficiency under different operating situations and optimization and designing of control systems . In past decades, several of PEM fuel cell models are defined to the purpose of gas channel, gas diffusion layers, catalyst layers and polymer membrane of electrolyte . Models can also be categorized based on their dimension, single, double or triple which can be considered either isothermal or non-isothermal [27]. Single cell model explain the electrochemical and transporting processes in the fuel cell component including pressure drop, flow distribution, and temperature profile in the gas channel. This simulation, quantitatively explain interaction between physical and electrochemical phenomenon which can also be divided into two sections, first an empirical simulation for prediction how the fuel cell voltages change with the current densities with polarization curves[28] and second principle simulation is built-up from ordinary differential equations or solving partial differential equations (PDEs) including distributed parameter, Stefan-Maxwell

convection and diffusion account for species conservation. Based on Darcy's law, the principle of mass conservation is applied to simulate reactant concentration. Recently, in advance simulation, two-dimensional and three dimensional simulations have been developed. The two-dimensional simulation can be separated into two classes, first one explain the plane perpendicular to the flow channels and second describes the direction along the flow channel [29,30]. An extended simulation of 3-dimensional, 2-phase, non-isothermal unit cell systems were investigated by Tao [28] for performing parameters sensitivities examination. Generally, simulated systems are lumped data of parameters for evaluating fuel cell efficiency under various operating situations for any controlling as a function of time through solving differential equations (ODEs). Pukrushpan [27] investigated a system including fuel cell stack, hydrogen supply, air supply, cooling and the humidification systems with a constant temperature due to the dynamics variables.

Computational details

Calculations were accomplished via GAMESS-US package [31]. DFT methods such as m062x, m06-L, and m06 for the non-bonded interaction of fuel cell layers including G_n // G_m have been used. The m062x, m06-L and m06-HF are new DFT functional with a good correspondence in non-bonded calculations which are useful for estimating the energies of distance between layers in the fuel cells simulation [32]. The double ζ-basis set with polarization orbitals (DZP) were applied for calculated for inputs and outputs parameters for the simulation fuel cells. Graphene is known to relax in 2-D honeycomb structures and the multi graphene also will be assumed to have a similar structure. A monolayer of graphene containing 76 atoms with zigzag edges was optimized and allowed to relax to its minimum energies structures. The edges were saturated with the hydrogen atoms for neutralizing the valance of terminal carbon, reducing the edge effect after relaxation. The C-C-C angle was calculated to be around 120.0 and the C-C and C-H bound lengths are about 1.422 and 1.086, respectively which are corresponds to reported paper [33]. The Perdew-Burke-Ernzerhof (PBE) [34] exchange-correlation (XC) functional of the generalized gradient approximation (GGA) is adopted. In our model, the electrodes have been doped by various percentages of boron atoms which are likely to be adjusted by the surrounding host C atoms. Therefore, when the graphene sheet is doped with one boron atom, the boron atom also undergoes the sp^2 hybridization. Using the computational procedure as stated above, the electronic properties, especially the band structure can be calculated. Via doping boron atoms in graphene, Fermi levels shifts significantly below the Dirac point resulting in a p-type doping. This would break the symmetry of graphene into two graphene sub-lattices due to

presence of the B atoms which would eventually lead towards a change of the behavior of graphene from semimetal to conductor which significantly is useful for fuel cells. The charge transfer and electrostatic potential-derived charge were also calculated using the Merz-Kollman-Singh [35], chelp [36], or chelpG [37]. We have also extracted the charge density profiles from first-principles calculation through an averaging process described.

Results & discussion

For the model of these fuel cells, the adsorption energies of various number of H_2, O_2 over the surfaces of multi graphene sheets have been calculated both in the anode and cathode plates (Figs.3).

Where BSSE is basis set error position. We obtain the stable situation after the modified system is fully relaxed. The activation energy barrier for O2 diffusion from graphene monolayer to graphene found to be as low as 0.05 eV.

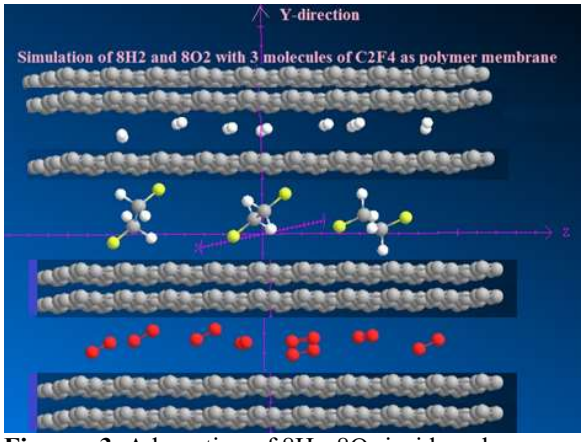

Figure 3. Adsorption of $8H_2$, $8O_2$ inside polymer membrane for a unit cell with multi layers graphene.

Initially, we assume that the adsorption is Langmuir uniformly both on graphene sheet. The adsorption energies can be calculated as follows:

$$E_{adsorb}^{H2} = \frac{1}{n}\left(E_{total} - E_{graphen} - nE_{H_2}\right) + E_{BSSE} \quad \textbf{(5)}$$

The barriers for the rest of the considered path are also quite low. The adsorption energies is are listed in table 2. The best simulation was found for 5; 5; 3 mole ratio of H_2, O_2 and polymer electrolyte (Table 2). For any further adsorption model, the validation of the Langmuir-Freundlich multilayer isotherm model is done using breakthrough experiments with binary mixtures of H_2/O_2, O_2/N_2 and H_2/H_2O (steam) and, a few component mixture composed by $H_2/O_2/H_2O/N_2$.

Table 2. The adsorption of H2 and N2 on surface of graphene

No. H_2	E_{adsorb}^{H2} *eV/H₂*	E_{adsorb}^{O2} *eV/O₂*	H_2 excess uptake (mg/g)
$1H_2$	-0.65	-0.36	39.1
$2H_2$	-0.58	-0.38	42.3
$3H_2$	-0.54	-0.44	41.4
$4H_2$	-0.61	-0.39	44.3
$5H_2$	-0.69	-0.48	45.6
$6H_2$	-0.57	-0.41	43.1
$7H_2$	-0.55	-0.43	42.2
$8H_2$	-0.51	-0.46	43.1
$9H_2$	-0.54	-0.42	41.2
$10H_2$	-0.56	-0.39	40.5

Breakthrough simulations are performed for different pressures, flow rates and different number molecules of adsorbent and also different sheets including graphite and monolayer graphene. The results are then compared with

experimental data from the literature. The Multisite Langmuir multilayer isotherm model and simulations with a four component mixtures of H_2/ O_2/H_2O/N_2 and are listed in table 3.

Adsorption strongly has been done σ-bonding orbitals of H2 molecule to the pi orbitals of C, B and N atom. While the back donation from the filled states of empty *d* orbitals to the *σ**-antibonding orbitals of H_2 molecule increase the interaction. Therefore the charge transfers are responsible for the elongation of H-H bond length in the H2 molecules and improve the adsorption abilities between those atoms of graphene sheets.

Table 3. K1,K2,K3 and K4 For H_2, N_2,O_2 and H_2O of Multisite Langmuir multilayer isotherm model

gas	K_1 Mol.Kg^{-1}.K^{-1}	K_2 Mol.Kg^{-1}. K^{-1}T^{-1}	K_3 atm^{-1}	K_4 K
Graphene (monolayer)				
H_2	16.9	-2*10^2	0.6*10^4	1200
N_2	1.7	-0.8*10^2	5*10^6	320
O_2	30.1	-9.0*10^2	2.1*10^4	-650
H_2O	27.5	-7.0*10^2	9*10^5	1002
Graphene (Bilayer)				
H_2	17.8	-2.5*10^2	1.4*10^4	1000
N_2	1.9	-1.5*10^2	5.5*10^6	450
O_2	30.5	-7.5*10^2	2.5*10^4	-620
H_2O	27.9	-8.0*10^2	8*10^5	882
Graphene (tetra layer)				
H_2	15.8	-2.0*10^2	2.1*10^4	1300
N_2	3.5	-1.9*10^2	3.5*10^6	850
O_2	21.8	-4.5*10^2	4.5*10^4	-420
H_2O	22.9	-5.0*10^2	8.7*10^5	500

Meanwhile, to exhibit the electronic distribution of system, the charge density differences of the systems are calculated for one to ten H2 molecules which are based on the following equation. $\rho = \rho_{H2,graphene} - \rho_{H2} - \rho_{graphene}$ where $\rho_{H2,graphene}$, ρ_{H2}, $\rho_{graphene}$ are the distribution of charge densities differences concerning adsorbing surfaces, isolated Hydrogen molecule, and monolayer graphene sheet, respectively. Based on these differences charges the electrical potential and differences voltages of 10 situations of H2 and O2 adsorption versus distance is shown in Fig.4. It clearly shows that on the surface of sheet, the electron density increases in the region between H2 molecule and B, N atoms .This means that H_2 molecule and graphene interact with each other, and there is also interaction between graphene sheet and O_2. In conclusion, multi layers plays an important role in the process of hydrogen storage.

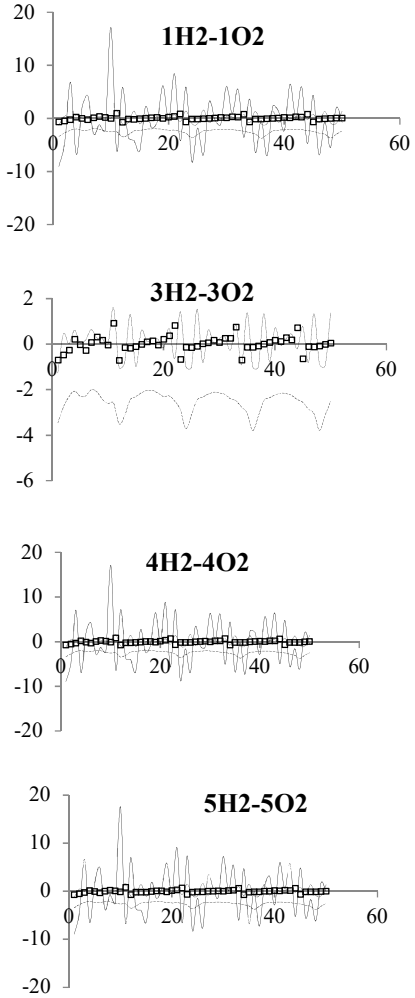

Figure 4. Electrical potential and difference voltages of 10 situations of H2 and O2 adsorption versus distance

Power density P of PEMFC in an irreversible path is depending on several variables including operating temperature T, working pressure a, proton exchange membrane water content λ or membrane water or membrane relative humidity ($\emptyset_m$) parameter and the proton membrane thickness d_{mem} and current density i, which can be expressed as $p = f(T, i, a, \lambda, d_{mem})$. It is important to keep some variables as a constant parameter such as working pressure a, the water content λ, and $d_{mem}$of, therefore the output power density is only a function of two variables i & T as $P= f(i, T)$. In isotherm of T, the output power densities of the irreversible PEMFC is function of current density, $P = f(i)$. When the operating temperature of the irreversible PEMFC is T_1, T_2, ….T_n the maximum output power densities are $P_{max}(1)$, $P_{max}(2)$, $P_{max}(n)$, respectively of an irreversible PEMFC in a finite time. Alike with the effect of $a, \lambda, and\ d_{mem}$ on its optimal output power density can also be discussed as same the above equation [Fig.5].

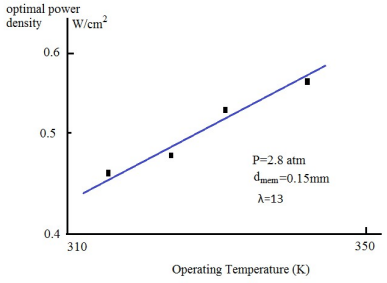

Figure 5. Optimal output power densities as a function of temperature.

It can be realized that the optimal output power densities of the irreversible PEMFC increase with the increasing of the operating temperature in the finite times. Obviously, due to the increase of T, the exchange current densities should be increased, the activation over potentials are reduced, and the proton pass rates have to be increased, as a result of the Ohmic over potentials and power dissipation are reduced. In small power dissipation, the minimum entropy production also decreases.

Consequently, increasing the operating temperature of the PEMFC can impressively develop its optimal output power densities in an appropriate working range. Increasing the operating pressure can also increase the density power of the irreversible PEMFC due to the increasing exchange current densities and decreasing activation over potential. Consequently the irreversibility of the irreversible PEMFC is diminished and the reversibility is elevated and the minimum entropies are decreased (Fig.6).

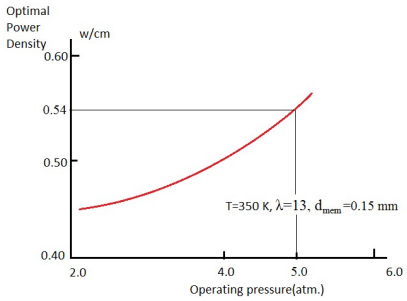

Figure 6. Optimal output power densities as a function of pressure.

As it can be seen corresponding optimal output power densities of pressures 3 and 4atm, are 0.46 and 0.505 W/cm^2, respectively. By increasing pressure from 3 atm. to 5 atm., the optimal output power densities are increased by 9.8% and also By increasing pressure from 4 atm. to 5 atm. the optimal output power densities are increased by 6.9% which means, the irreversible PEMFC can

further improve its optimal output power density by suitably increasing its operating pressure during finite time operations.

Our calculation exhibits a maximum output power density through increasing the proton membrane thickness and this phenomenon is due to increase the hindrance of ions via the proton exchange membrane. Simultaneously, the Ohmic loss has been growth, the output power densities are decreased, and the maximum output power is also decreased (Fig.6).

Conclusion

We have accomplished first-principles electronic structure calculations for studying the amount of hydrogen storage and oxygen diffusion on the graphene sheets. A stable and uniform Longmuir adsorption of H2 on graphene can be done . We find the stable geometry configurations of H_2 molecules absorbed on graphene sheet . The modified system can absorb 5H2 molecules with the maximum adsorption energy -0.69 eV/H2 which meets the ideal adsorption energy for H2 molecules to be recycled at near ambient conditions. This work displays the outstanding potential to become one of suitable method for hydrogen storage.

References

[1] Ciureanu M, Effects of nafion dehydration in pem fuel cells. Journal of AppliedElectrochemistry, 2004; 34(7):705-714

[2] Cruz-Manzo S, Chen R, Rama P. Study of current distribution and oxygen diffusion in the fuel cell cathode catalyst layer through electrochemical impedance spectroscopy. International Journal of Hydrogen Energy, 2013; 38(3):1702- 1713

[3] de Bruijn FA, Dam VAT, Janssen GJM. Review: Durability and degradation issues of PEM fuel cell components. Fuel Cells, 2008; 8(3), 22

[4] Larminie J, Dicks A. Fuel Cell Systems Explained. J. Wiley, 2003

[5] Inc. Science Applications International Corporation Parsons. Fuel cell Handbook. U.S. Department of Energy, 2000

[6] Kazmi, I H, Bhatti A I, Iqbal S. A nonlinear observer for pem fuel cell system.Multitopic Conference, 2009, INMIC, 2009; IEEE 13th International, pages 1-6

[7] U.S. Department of Energy. Hydrogen Data Book , 2017. Accessed on March 17th, 2017.

[8] Litster S, McLean G. PEM fuel cell electrodes. Journal of Power Sources, 2004; 130(1):61, 76

[9] Schmittinger W, Vahidi A, A review of the main parameters influencing longterm performance and durability of PEM fuel cells. Journal of Power Sources, 2008; 180(1):1- 14

[10] Borup R et al, Scientific aspects of polymer electrolyte fuel cell durability and degradation. *CHEMICAL REVIEWS*, 2007; 107(10), 3904{3951

[11] Fly A. Thermal and water management of evaporatively cooled fuel cell vehicles. PhD thesis, Loughborough University, UK, 2015.

[12] Zawodzinski T A, Derouin C, Radzinski S, Sherman R J, Smith V T, Springer T E, Gottesfeld S. Water uptake by and transport through nafion membranes. 1993; 140(4):1041-1047

[13] Su A, Weng F, Hsu C, Chen Y. Studies on flooding in PEM fuel cell cathode channels. International Journal of Hydrogen Energy, 2006; 31(8):1031- 1039, 2006.

[14] Pasaogullari U,Wang C, Two-phase modeling and flooding prediction of polymer electrolyte fuel cells. Journal of The Electrochemical Society, 2005; 152(2): 380-390

[15] Futerko P, Hsing I, Two-dimensional finite-element method study of the resistance of membranes in

polymer electrolyte fuel cells, 2000; Electrochimica Acta, 45(11):1741-1751

[16] Dutta S, Shimpalee S, Van Zee J W. Three-dimensional numerical simulation of straight channel pem fuel cells. Journal of Applied Electrochemistry, 2000, 30(2):135-146

[17] Wang Z H, Wang C Y, Chen K S, Two-phase flow and transport in the air cathode of proton exchange membrane fuel cells. Journal of Power Sources, 2001, 94(1):40- 50

[18] He W, Lin G, Van Nguyen T, Diagnostic tool to detect electrode flooding in proton-exchange-membrane fuel cells. AIChE Journal, 49(12)

[19] Bosco A D P, Fronk M H, Fuel cell flooding detection and correction, 2000. US Patent 6,103,409.

[20] Le Canut J, Abouatallah R M, Harrington D A, Detection of membrane drying, fuel cell flooding, and anode catalyst poisoning on pemfc stacks by electrochemical impedance spectroscopy, 2006; 153(5): 857-864

[21] Ciureanu M, Effects of nafion dehydration in pem fuel cells. Journal of Applied Electrochemistry, 2004; 34(7):705-714

[22] Frano Barbir. PEM Fuel Cells: Theory and Practice. Academic Press, 2005

[23] Andrew Hamnett Carl H Hammann and Wolf Vielstich. Electrochemestry, WileyVCH, 2007

[24] Rowe A, Li X. Mathematical modeling of proton exchange membrane fuel cells, Journal of Power Sources, 2001; 102(1):82-96

[25] Siegel C. Review of computational heat and mass transfer modeling in polymerelectrolyte-membrane (pem) fuel cells. Energy, 2008; 33(9):1331-1352

[26] Yao K Z,. Karan K, McAuley K B, Oosthuizen P, Peppley B, Xie T, A review of mathematical models for hydrogen and direct methanol polymer electrolyte membrane fuel cells. Fuel Cells, 2004; 4(1), 3-29

[27] Pukrushpan J T, Peng H, Stefanopoulou A G, Control-oriented modeling and analysis for automotive fuel cell systems. Journal of Dynamic Systems, Measurement, and Control, 2004, 126:14

[28] Tao W Q, Min C H, Liu X L, He L Y, Yin B H, Jiang W, Parameter sensitivity examination and discussion of PEM fuel cell simulation model validation: Part i. current status of modeling research and model development. Journal of Power Sources, 2006, 160(1):359-373

[29] Karimi G et al. Along-channel flooding prediction of polymer electrolyte membrane fuel cells. International Journal of Energy Research, 2011, 35(10):883-896

[30] Gurau V et al. Two-dimensional model for proton exchange membrane fuel cells. AIChE Journal, 1998, 44(11):2410- 2422

[31]. Schmidt MW, Baldridge kk, Boatz JA, Elbert ST, Gordon Ms, Jensen JH, Koseki S, Matsunaga N, Nguyen KA et al General atomic and molecular electronic structure system. J Compt chem 2004; 14(11): 1347–1363

[32]. Zhao Y, Truhlar DG (2008) The M06 suite of density functional for main group thermochemistry, thermochemical kinetics, non-covalent interactions, excited states, and transition elements: two new functional and systematic testing of four M06-class functional and 12 other functional. Theor Chem Account 2008; 120:215–241

[33] Ao Z, Yang J, Li S, Jiang Q, Enhancement of CO detection in Al doped graphene. ChemPhys Lett, 2008, 461(4):276-279

[34] Perdew J P, Burke K and Ernzerhof, Generalized Gradient Approximation Made Simple. Phys. Rev. Lett, 1996, (77): 3865-3868

[35]. Besler BH, Merz KM, Kollman PA (1990) Atomic charges derived from semi empirical methods J. comp. Chem (11): 431-439,

[36]. Chirlian LE, Francl MM (1987) Atomic charges derived from electrostatic potentials: A

detailed study. J.comp.chem (8): 894-905,

[37]. Brneman GM, Wiberg KB (1990) J. Comp Chem (11): 361